CONF-890426--20

MAGNETO-OPTICAL PROPERTIES OF ULTRATHIN FERROMAGNETIC FILMS*

CONF-890426--20

DE89 014640

S. D. Bader, E. R. Moog, C. Liu, and J. Zak**

Materials Science Division

Argonne National Laboratory, Argonne, Illinois 60439

April 1989

Manuscript submitted to MRS Spring Meeting, Symposium on Magneto-Optic Data San Diego, CA, April 24-29, 1989, Sponsored by the Materials Research Society.

---

*Work supported by the U.S. Department of Energy, BES-Materials Sciences, under contract #W-31-109-ENG-38 (Argonne).

**Permanent address: Phys. Department, Technion, Haifa, Israel.

MAGNETO-OPTICAL PROPERTIES OF ULTRATHIN FERROMAGNETIC FILMS

S. D. BADER, E. R. MOOG, C. LIU, AND J. ZAK*
Materials Science Division, Argonne National Laboratory
Argonne, Illinois 60439

ABSTRACT

The surface magneto-optic Kerr effect (SMOKE) has been used to explore the properties of ultrathin ferromagnetic films. The ultrathin regime corresponds to thicknesses less than the depth penetration of light and includes the monolayer range. The ultrathin regime possesses unique magneto-optic properties: the Kerr rotation and ellipticity, in general, behave differently than in the thick film limit. Measurements and simulation in the longitudinal geometry for bcc Fe on Au(100) provide a dramatic example of the metallic reflector enhancement effect due to the nonmagnetic Au underlayer. The rotation enhancement is accompanied by a high reflectivity, as opposed to being at the expense of the reflectivity. Measurements in both polar and longitudinal geometries for epitaxially-stabilized fcc Fe films grown on Cu(100) and Pd(100) indicate the presence of perpendicular surface anisotropy, which suggests new approaches to realizing vertical data-storage media.

INTRODUCTION

The magneto-optical Kerr effect has recently proven to be a powerful probe of the magnetic properties of ultrathin ferromagnetic films.[1-7] Such films are fabricated by epitaxial deposition of magnetic elements, such as Fe, onto non-magnetic, single-crystal substrates in ultra-high vacuum. The ultrathin regime corresponds to Fe thicknesses less than the depth penetration of light and includes the monolayer and submonolayer range. It is possible to create new and metastable phases and to alter the lattice constants of equilibrium phases via epitaxial deposition.[8-10] Also, the magnetic properties at surfaces and interfaces are unique because of the reduced coordination and the loss of translational symmetry perpendicular to the plane of the film.[11,12] Thus, there are many materials challenges that make the field rich with opportunities.

In addition to the fascinating possibilities concerning the magnetic properties, the magneto-optical response itself becomes a challenge to understand in the ultrathin limit. In the present work we summarize our recent efforts in this area. We use the acronym we introduced in 1985 to identify our studies: SMOKE for the surface magneto-optic Kerr effect.[1] We will see that there are profoundly intriguing characteristics of the SMOKE signals that differentiate them from the conventional Kerr-effect response. The ultrathin regime might provide a basis for the technological development[13,14] of a future generation of materials for magneto-optic data storage. This is because desirable properties of surfaces and interfaces potentially can be retained in sandwich and superlattice geometries that serve to protect the reactive magnetic layers, while enhancing their optical characteristics.[15-17]

In the following we survey some of the ideas that might be fruitful for further development. We consider first the longitudinal Kerr effect. We present data for Fe grown on Au(100) between 0-400 Å, and show that in the ultrathin regime the rotation and ellipticity behave differently than in the thick-film limit. We then present simulations based on published optical constants to understand the origin of the differences. The simulations provide a dramatic example of the metallic reflector enhancement effect due to the non-magnetic Au underlayer. Finally, we outline some recent SMOKE results in the polar configuration to demonstrate that the surface magnetic anisotropy can provide a new way to realize vertical magneto-optic media.

BACKGROUND

Materials Aspects

The experimental configuration involves an ultra-high vacuum (UHV) chamber separated from the optical components by a UHV window. The base pressure of the vacuum system is 10^{-11} Torr, which is necessary in order to preserve the atomic cleanliness of the surfaces under study. Single crystals of Au(100) or other substrates are prepared in-situ by sputter-anneal cycles and monitored before and after Fe deposition using low-energy electron diffraction (LEED) and Auger electron spectroscopy. LEED is used to verify the epitaxy, and Auger is used to monitor the cleanliness and growth mode, as described elsewhere.[1-5] The Fe is lattice matched to grow on Au(100) in a relatively unstrained bcc phase. This is because the bulk-terminated Au(100) face forms a square net of lattice constant 2.88 Å, which is similar to the 2.87-Å lattice constant of bcc Fe. It is also possible to grow metastable fcc Fe using substrates such as Cu(100) and Pd(100). The mismatch in lattice constant between fcc Fe and these substrates is expected to produce a tetragonal distortion perpendicular to the plane of the film, which should be particularly pronounced for Fe on Pd as compared to Fe on Cu.[10]

The epitaxy for Fe on Au gives rise to well-ordered LEED beams because the Au substrate is held at elevated temperatures (~200°C) during deposition. The elevated temperature, however, promotes diffusion and permits a monolayer of Au to segregate to the surface of the Fe film to lower the surface free energy of the system. For Fe deposition on the other film systems the substrate was held at room temperature or below to suppress segregation and intermixing at the interface. These materials preparation and characterization details are outlined in greater detail in other publications.[1-5,10] For the present purposes the most important feature to emphasize is that single crystalline films are grown in a relatively well ordered, layer-by-layer growth fashion.

The easy axes of magnetization can be in-plane or perpendicular to the plane of the film.[18] In-plane orientations are expected due to the shape of the films. Perpendicular orientations can arise from the surface magnetic anisotropy contributions.[12] If perpendicular surface anisotropy is present, it would only persist to a critical thickness, above which the magnetization orientation would reorient in-plane. It is found that the easy axis is in-plane for Fe/Au(100),[1,19] but can be perpendicular[10] for Fe on Cu(100) or Pd(100), as will become apparent. The films are generally characterized by low-coercivity values, e.g., <10 Oe for Fe/Au(100) and <1 kOe for Fe/Cu(100). This makes it particularly straightforward to incorporate miniature electromagnets in the vacuum chamber to magnetize or reverse the magnetization of a film. For the

perpendicular surface anisotropy studies a crossed magnet configuration is utilized so that in-plane and perpendicular fields can be applied sequentially.

Magneto-Optical Aspects

Longitudinal magneto-optical measurements were undertaken for Fe/Au(100). The basic optical configuration consists of a He-Ne laser source shining through the UHV window and reflecting off the magnetized film. (The angle of incidence is 22° due to physical constraints that prevented a larger value.) The reflected light passes back through the window, and through a polarizing crystal analyzer (set 2.35° off of extinction) to a photodiode detector. Magnetic hysteresis loops are derived by sweeping the field and monitoring the detector output with a laboratory computer programmed to signal average multiple scans. Kerr rotations can then, in principle, be derived from the intensity data.[5] The advantage is that mechanical adjustments are unnecessary, and small-signal detection is possible even into the submonolayer regime. The problem is that the birefringence of the UHV window interconverts rotation ϕ and ellipticity ε, and prevents accurate rotation measurements. The solution to the problem that we chose is to use two Babinet-Soleil compensators in a configuration that permits measurements of the magnitude of the complex rotation ϕ_m without interference from the window, where

$$\phi_m = \sqrt{\phi^2 + \varepsilon^2}$$

The procedure is outlined elsewhere along with accompanying algebraic[20] and geometric[5] descriptions in terms of operations on the Poincaré sphere. The bonus, we realized in hindsight, is that ϕ and ε could be reconstructed from the known compensator settings.[20] Although the error bars in the analysis suggest that there must be better ways to proceed in the future, the methodology provides us with the first systematic glimpse of the magneto-optical behavior in the ultrathin regime.

Polar Kerr-effect measurements were made on systems such as Fe on Cu(100) and Pd(100) to search for perpendicular surface anisotropy.[10] Since the issues associated with these studies are qualitative in nature (i.e., is the easy axis parallel or perpendicular?) and since monolayer-range signals are inherently small, no effort was made to separate ϕ from ε. Generally, a compensator or quarter-wave plate would be inserted between the window and analyzer to improve the signal strength; no further adjustments would then be attempted in the coarse of the experiments.

Computational Aspects

Values of ϕ, ε, ϕ_m and of the reflectivity R were calculated using the formulas of Yoshino and Tanaka[21] and the magneto-optical coupling constant Q reported by Krinchik and Artem'ev.[22] The formulation involves using Snell's law and the Fresnel coefficients to calculate the quantities of interest. The inputs include the Fe thickness and the angle of incidence θ, and the complex index of refraction of Fe and of Au n_{Fe} and n_{Au}, respectively, and the complex magneto-optic coupling constant Q of Fe at the He-Ne wavelength.

The Fe thickness d is treated as a variable to calculate the thickness dependences of interest. Alternately, θ dependences can be calculated for a fixed d, but these results are of less interest here, since they show qualitatively similar trends to those already established for thicker films.[23] The computational problem is related to those treated recently for the polar Kerr effect of Fe-Cu bilayered films and superlattices of variable bilayer thickness,[24-26] and by Dillon, et al.[27] for the longitudinal Kerr effect of thick magnetic films (permalloy) buried under varying thicknesses of nonmagnetic material (Nb).

RESULTS AND DISCUSSION

Thickness Dependent of ϕ_m

The magnitude of the complex rotation ϕ_m is shown in Fig. 1 as a function of Fe thickness for Fe/Au(100). Data are presented for both s- and p-polarized light, but a single smooth curve is drawn through the data to emphasize the similarities. There are three distinct characteristics of the data to emphasize. Firstly, the signal initially increases linearly with thickness. Secondly, it goes through a shallow maximum at intermediate thickness. Finally, it approaches a constant value in the thick-film limit. This immediately points to the relevance of the SMOKE acronym as distinct from conventional MOKE, since the Kerr effect traditionally is defined as being independent of thickness, while the Faraday effect is proportional to thickness. Here we see that the SMOKE signal is initially proportional to thickness, as in the Faraday effect.

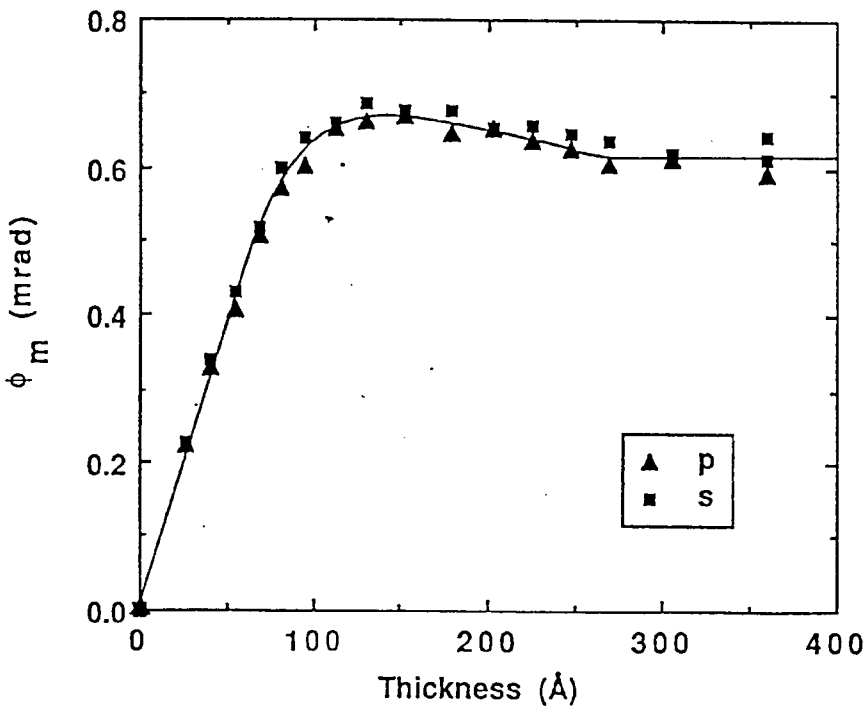

Fig. 1. The measured magnitude of the complex magneto-optic rotation ϕ_m as a function of Fe thickness for Fe/Au(100). The smooth curve serves as a guide to the eye.

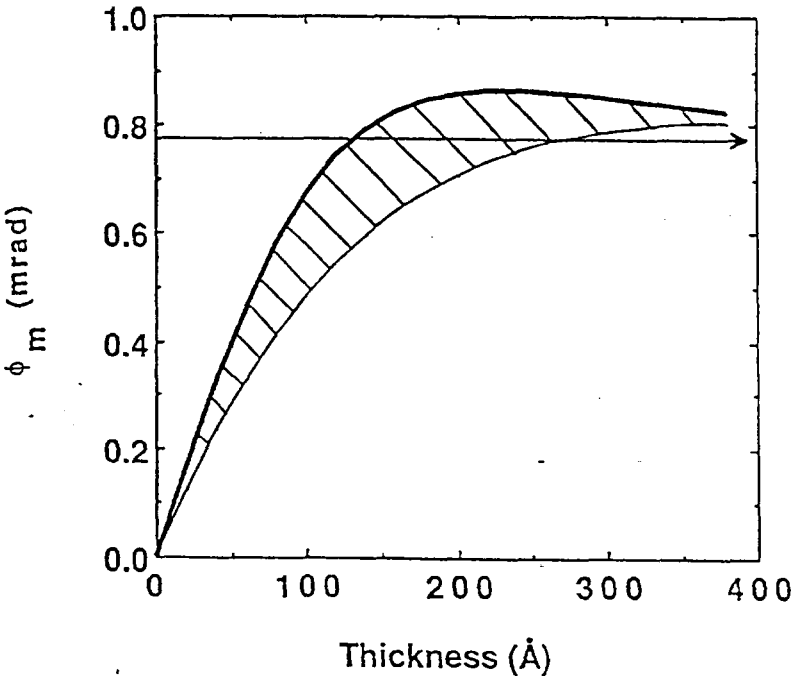

Fig. 2. The calculated ϕ_m as a function of Fe thickness for Fe/Au (bold curve) and Fe simulated on non-magnetic Fe (light curve). The hatched area shows the enhancement due to the Au reflector. The horizontal line indicates the thick-film limiting value of ϕ_m calculated for pure Fe.

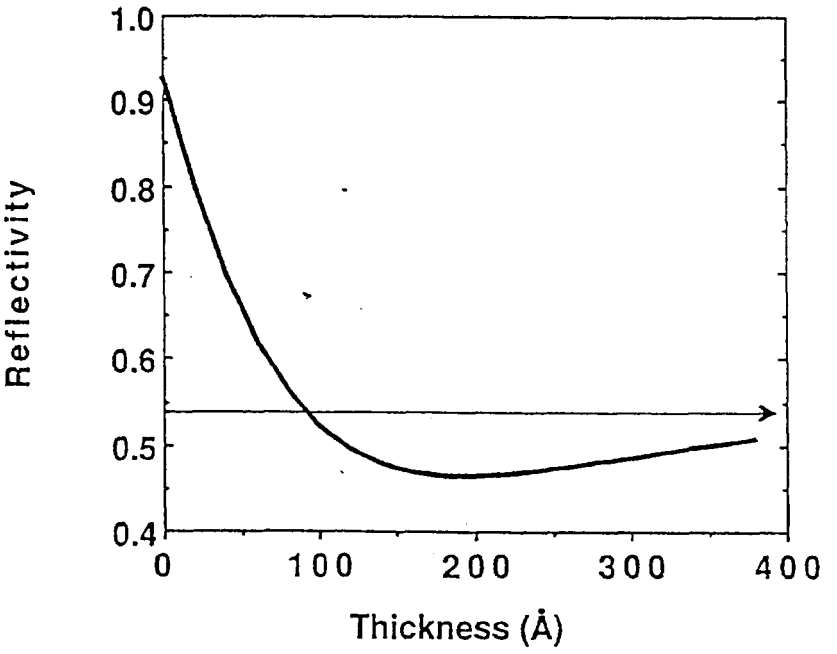

Fig. 3. The calculated reflectivity as a function of Fe thickness for Fe/Au. The horizontal line indicates the thick-film limiting value calculated for pure Fe.

To explore the issue further, simulations were performed using published optical data for Fe and Au. The calculated thickness dependence of ϕ_m for p-polarized light is shown in Fig. 2 by the heavy-line curve. The thick-film limiting ϕ_m value for pure Fe is denoted by the horizontal line that is

terminated by an arrow. The three distinct features observed in the experimental data are reproduced in the calculation. There is an initial linear rise, a broad, shallow peak, and a gradual approach to the thick-film limiting ϕ_m value. There are quantitative differences between experiment and calculation, but the same qualitative trends are present in both.

The corresponding reflectivity calculation appears in Fig. 3, where the curve is for Fe on Au, and the horizontal line is the (p-polarized) reflectivity of pure Fe, for comparison. The shallow peak in the ϕ_m calculation of Fig. 2 is seen to be associated with the broad reflectivity minimum of Fig. 3. The reflectivity decreases from the pure Au value, goes through a minimum, and recovers to the pure Fe value as the film thickness becomes comparable to the depth penetration of the light. The high reflectivity of the Au causes a strong back-reflection of the beam that was transmitted through the Fe film. Thus, the initial linear increase in the ϕ_m occurs in the transition region between the double Faraday regime and the conventional Kerr regime. This simple picture provides a useful description, despite the semantic distinctions.

To provide further insights, another calculation was performed as shown by the light-line curve in Fig. 2. The complex index of refraction of Au was replaced by that of Fe, so that R becomes independent of thickness. Thus, magnetic Fe is grown on a non-magnetic Fe substrate. The reflectivity match at the interface gives less back-scattering, so the signal increases initially at a slower rate than previously. The shallow maximum is extremely weak and is shifted out to a higher thickness value that is off scale.

Enhancement Effects

The hatched area in Fig. 2 shows the region of enhanced magneto-optical response due to the Au reflector enhancement effect. This effect has been discussed previously,[28,29] but Fig. 2 provides a particularly clear simulation of the effect. It is this effect that gives rise to the enhancements reported for Fe-Cu bilayers and superlattices.[24-26] The appealing feature of the enhancement from a device perspective is that it is accompanied by a strong reflectivity, rather than being at the expense of the reflectivity. This is important since the figure of merit for data-storage applications involves a multiplicative function of the rotation and reflectivity.[13] The enhancement effect should be applicable to a broad range of materials systems, and in the polar as well as in-plane magnetization configurations. The particular system under consideration, Fe/Au, is not a candidate for applications, however, since among other factors, the coercivities are too low.

Rotation and Ellipticity Behavior

Figure 4 shows the behavior of the rotation and ellipticity as a function of thickness, as analyzed from experimental data, such as appear in Fig. 1. The ϕ and ε values are reconstructed using the compensator settings, as described in the previous section, and in more detail elsewhere.[20] Rotation results in Fig. 4a show that the s- and p-polarized signals are similar, except that they are of opposite sign, as expected. Most importantly they both have very small values between 0 to ~30 Å. The ellipticity, on the other hand, initially has a strong linear increase, goes through a pronounced maximum at ~100 Å and levels off to a thick-film limiting value of about half the peak

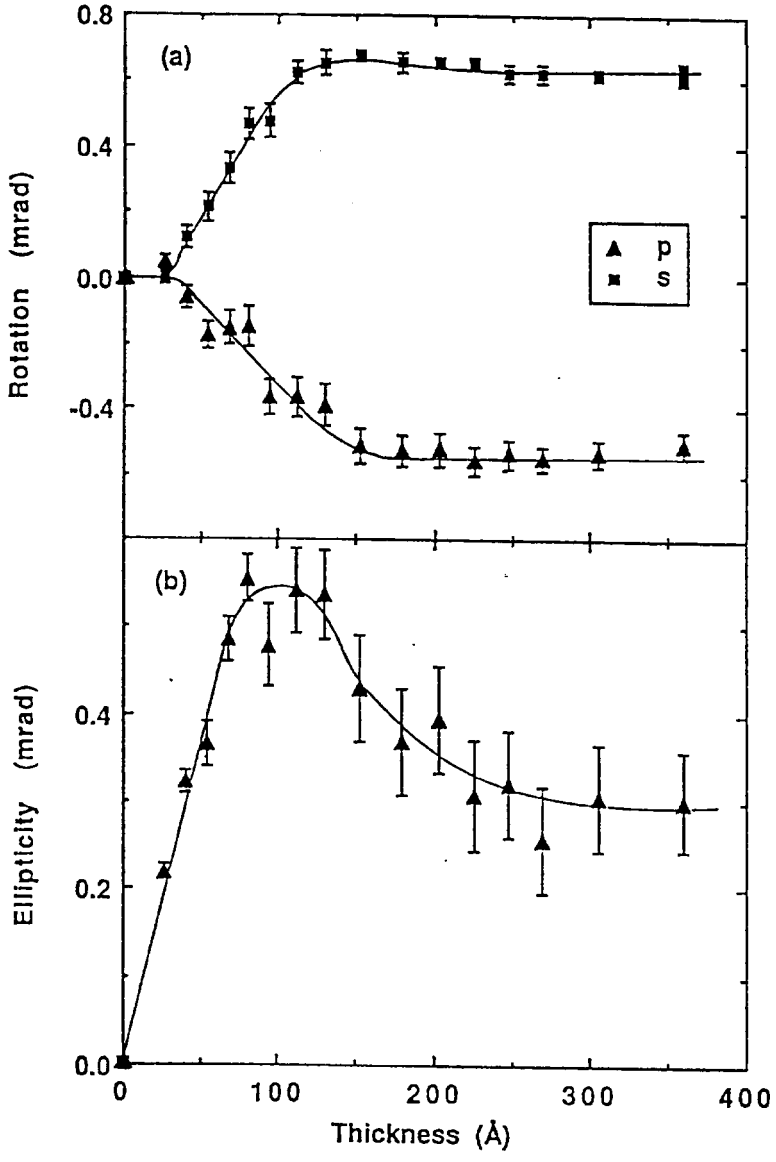

Fig. 4. The experimental rotation (a) and ellipticity (b) values derived for Fe/Au(100) from the ϕ_m values and compensator settings. The smooth curves serve as guides to the eye.

value. This shows that the initial rise in ϕ_m is dominated by ε, while in the thick-film limit ϕ is known to dominate ϕ_m. This type of behavior is another distinguishing characteristic of the SMOKE signal as compared to the conventional response. The component contributions interfere and are phase shifted to produce the unusual effects observed in Fig. 4.

To demonstrate that the peculiarities of Fig. 4 are not artifacts of the data-analysis methodology, we present in Fig. 5 simulations of the quantities of interest using bold curves, along with the calculated thick-film limiting values using arrowed horizontal lines. The calculated rotation in Fig. 5a is very small between approximately 0-30 Å, as in the experiment of Fig. 4a. The calculated ellipticity in Fig. 5b initially has a strong linear increase, a pronounced maximum at ~125 Å, and a limiting value of about half the peak value, all in accord with the experimental trends in Fig. 4b. These results demonstrate the utility of the simulations to yield guidelines that are realistic on a qualitative and even semi-quantitative scale. This is done without

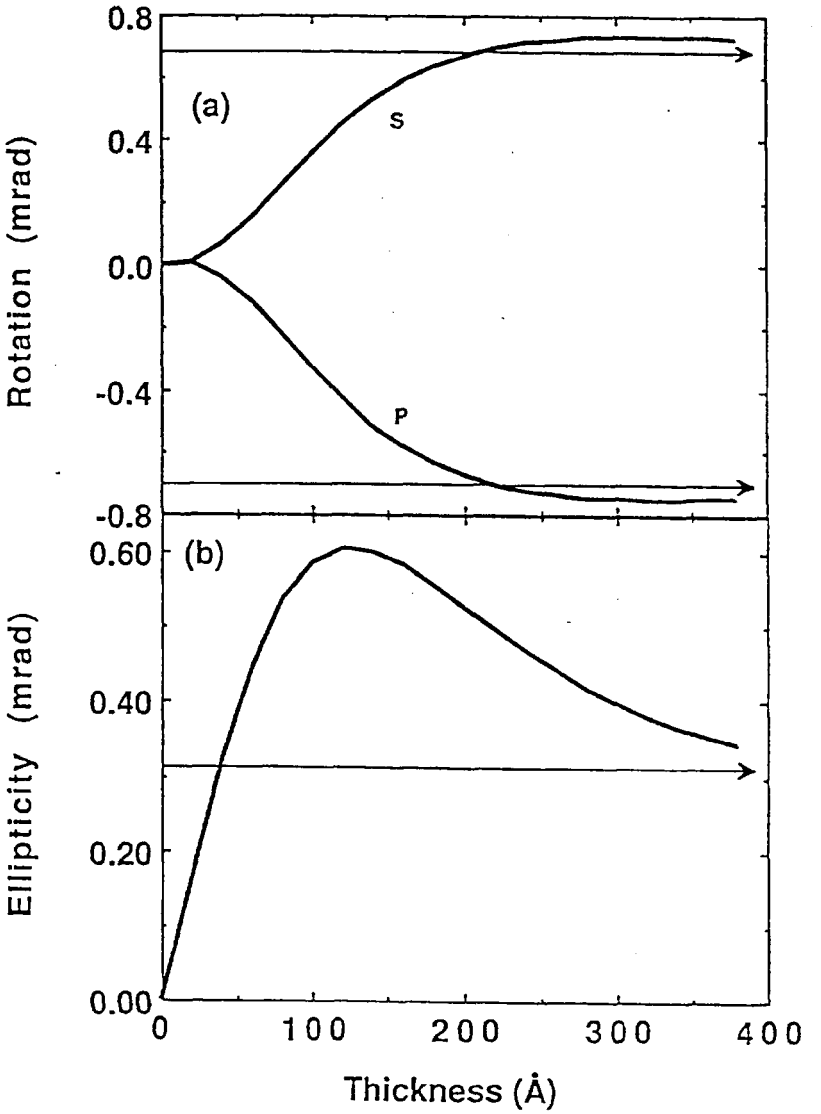

Fig. 5. The calculated rotation (a) and ellipticity (b) values simulated for Fe/Au as a function of Fe thickness, along with the limiting values (horizontal lines) calculated for pure Fe.

refining the tabulated optical parameters in any way. There are reports of thickness dependent indices of refraction for thin films,[30] and there is also the well-known expectation that electronic and optical properties at surfaces and interfaces can be different than bulk properties. So there are reasons to expect that simple models will break down. However, the present modeling effort suggests that the break down is only quantitative in nature for the present system. Much more detailed theoretical modeling will be necessary, as is presently being pursued for bulk materials,[31] to fully appreciate the role of surfaces and interfaces.

Perpendicular Surface Anisotropy

Surface properties become much more apparent in controlling the magneto-optical behavior for the systems Fe/Cu(100) and Fe/Pd(100). For each of these systems we have found that perpendicular easy axes can be realized under the proper growth conditions up to a critical thickness that ranges from ~6 monolayers for Fe/Cu(100) to <3 monolayers Fe for Fe/Pd(100), as

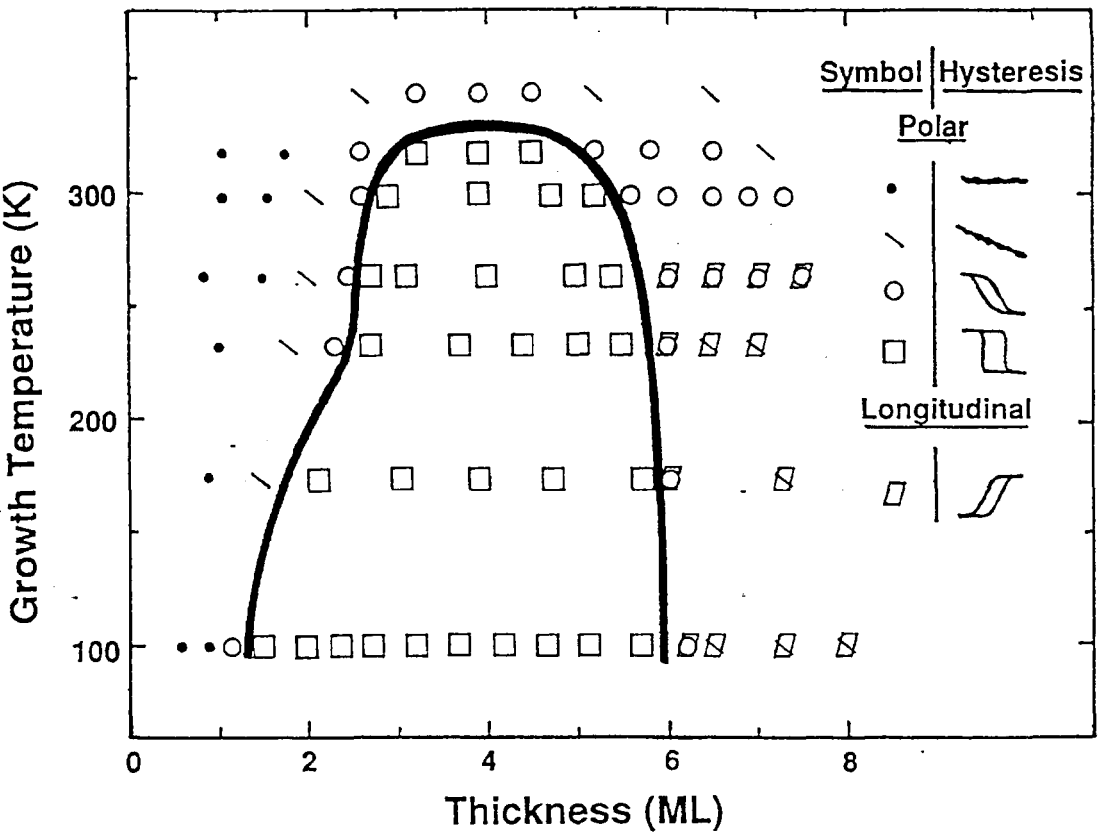

Fig. 6. The region of stability of perpendicularly-oriented square loops for fcc Fe/Cu(100) is delineated on a plot of film thickness vs. growth temperature. The measurements were made at the growth temperature.

shown in Figs. 6 and 7, respectively. Also, the polar Kerr signal has the additional advantage that it is stronger than the longitudinal signal. It is expected that it will be possible to retain some of these desirable surface properties in sandwich and superlattices configurations involving non-magnetic layers that protect the reactive magnetic layers and that tailor their optical response.

SUMMARY

The present work surveyed recent results obtained on our laboratory on magneto-optics of ultrathin films. We presented longitudinal Kerr-effect measurements for Fe on Au(100) and compared to computer simulation using published optical data to understand the nature and origin of the signal in the 0-400 Å region of Fe thickness. The Au reflector enhancement effect was noted, as well as interesting interference effects between Kerr and Faraday channels, and rotation and ellipticity channels. Perpendicular surface magnetic anisotropy was briefly mentioned, as well. Due to the advent of modern ultra-high vacuum technology it appears quite fruitful to systematically pursue the issues raised by the ultrathin limit. There is basic as well as technological interest. The field of 'atomic' engineering of magnetic and magneto-optical materials may be right on the horizon.

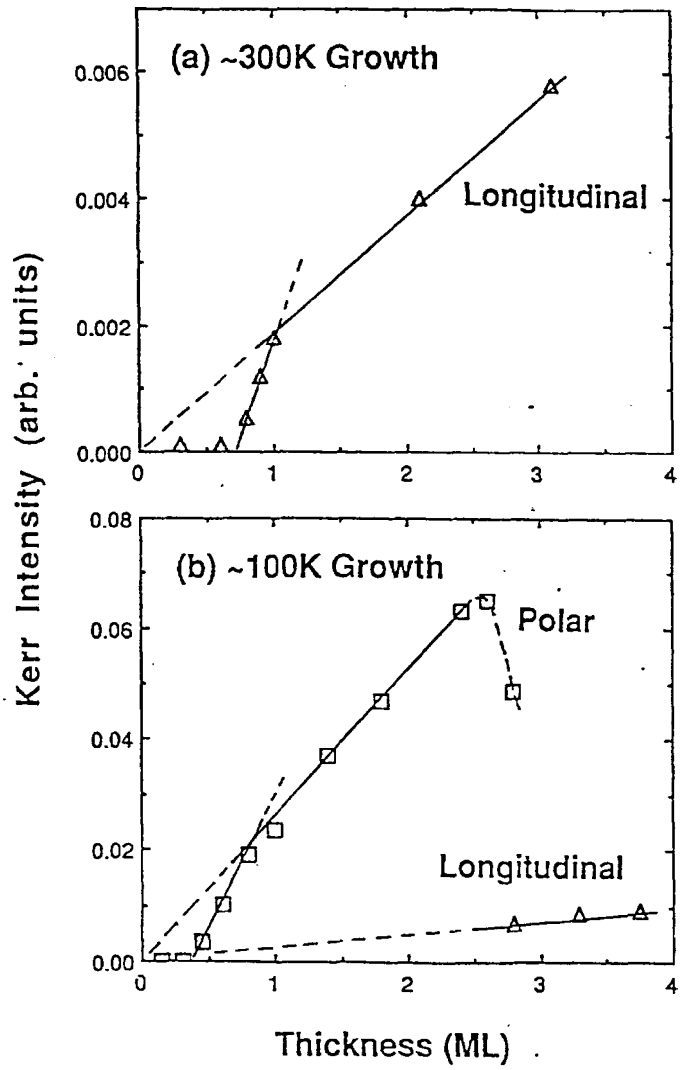

Fig. 7. Magnetic anisotropy data measured at the growth temperature are shown for Fe/Pd(100) at (a) ~300 K and (b) ~100 K. Note that vertical spin orientations are not stable for 300-K growth, and that the critical thickness for vertical easy axes is <3 monolayers for ~100-K growth. The Kerr intensity refers to the height of the hysteresis loop obtained from the photodiode detector.

ACKNOWLEDGMENT

We thank J. Pearson for technical assistance. This work was supported by the U.S. Department of Energy, BES-Materials Sciences, under contract #W-31-109-ENG-38.

REFERENCES

* Permanent address: Physics Department; Technion; Haifa, Israel.

1. E. R. Moog and S. D. Bader, Superlattices Microstruct. 1, 543 (1985); S. D. Bader, E. R. Moog, and P. Grünberg, J. Magn. Magn. Mater. 53, L295 (1986).
2. S. D. Bader and E. R. Moog, J. Appl. Phys. 61, 3729 (1987).
3. P. A. Montano, G. W. Fernando, B. R. Cooper, E. R. Moog, H. M. Naik, S. D. Bader, Y. C. Lee, Y. N. Darici, H. Min, and J. Marcano, Phys. Rev. Lett. 59, 1041 (1987).
4. C. Liu, E. R. Moog, and S. D. Bader, Phys. Rev. Lett. 60 2422 (1988); J. Appl. Phys. 64, 5325 (1988).
5. E. R. Moog, C. Liu, S. D. Bader, and J. Zak, Phys. Rev. B 39, 6949 (1989).
6. T. Beier, H. Jahrreiss, D. Pescia, Th. Woike, and W. Gudat, Phys. Rev. Lett. 61, 1875 (1988).
7. J. Araya-Pochet, C. A. Ballentine, and J. L. Erskine, Phys. Rev. B 38, 7846 (1988).
8. G. A. Prinz, Phys. Rev. Lett. 54, 1051 (1985).
9. A. S. Arrott, B. Heinrich, S. T. Purcell, J. F. Cochran, and K. B. Urquhart, J. Appl. Phys. 61, 3721 (1987).
10. C. Liu and S. D. Bader, Physica B (to be published).
11. C. L. Fu, A. J. Freeman, and T. Oguchi, Phys. Rev. Lett. 54, 2700 (1985).
12. J. G. Gay and R. Richter, Phys. Rev. Lett. 56, 2728 (1986).
13. M. H. Kryder, J. Appl. Phys. 57, 3913 (1985).
14. K. Tsushima and N. Koshizuka, IEEE Trans. Magn. MAG-23, 3473 (1987).
15. C. H. Lee, H. He, F. Lamelas, W. Vavra, C. Uher, and Roy Clarke, Phys. Rev. Lett. 62, 653 (1985).
16. F. J. A. den Broeder, D. Kuiper, A. P. van de Mosselaer, and W. Hoving, Phys. Rev. Lett. 60, 2769 (1988).
17. A. Boufelfel, B. Hillebrands, G. I. Stegeman, and C. M. Falco, Solid State Commun. 68, 201 (1988).
18. U. Gradmann, J. Magn. Magn. Mater. 54-57, 733 (1986).
19. W. Dürr, M. Taborelli, O. Paul, R. Germar, W. Gudat, D. Pescia, and M. Landolt, Phys. Rev. Lett. 62, 206 (1989).
20. E. R. Moog, J. Zak, M. L. Huberman, and S. D. Bader, Phys. Rev. B (to be published).
21. T. Yoshino and S. Tanaka, Jpn. J. Appl. Phys. 5, 989 (1966).
22. G. S. Krinchik and V. A. Artem'ev, Sov. Phys. JETP 26, 1080 (1968).
23. J. H. Judy, IEEE Trans. Magn. MAG-6, 563 (1970).
24. T. Katayama, Y. Suzuki, H. Awano, Y. Nishihara, and N. Koshizuka, Phys. Rev. Lett. 60, 1426 (1988).
25. T. Katayama, Y. Nishihara, and H. Awano, J. Appl. Phys. 61, 4329 (1987).
26. K. Sato, H. Kida, and T. Katayama, Jpn. J. Appl. Phys. 27, L237 (1988).
27. J. F. Dillon, Jr., E. M. Gyorgy, F. Hellman, L. R. Walker, and R. C. Fulton, J. Appl. Phys. 64, 6098 (1988).
28. A. J. Kolk and M. Orlovic, J. Appl. Phys. 34, 1060 (1963).
29. J. H. Judy, J. K. Alstad, G. Bate, and J. R. Wiitala, IEEE Trans. Magn. MAG-4, 401 (1968).
30. J. Kranz and H. Stremme, IEEE Trans. Magn. MAG-5, 453 (1969).
31. G. H. O. Daalderop, F. M. Mueller, R. C. Albers, and A. M. Boring, Appl. Phys. Lett. 52, 1639 (1988); J. Magn. Magn. Mater. 74, 211 (1988).